Environmental Science Processes & Impacts

ROYAL SOCIETY OF CHEMISTRY

PAPER

View Article Online
View Journal | View Issue

Cite this: *Environ. Sci.: Processes Impacts*, 2022, **24**, 426

Spatial distribution and biogeochemistry of redox active species in arctic sedimentary porewaters and seeps†

Jeffrey M. Hudson,[a] Alexander B. Michaud,[b] David Emerson[b] and Yu-Ping Chin *[a]

Received 2nd December 2021
Accepted 3rd February 2022

DOI: 10.1039/d1em00505g

rsc.li/espi

Redox active species in Arctic lacustrine sediments play an important, regulatory role in the carbon cycle, yet there is little information on their spatial distribution, abundance, and oxidation states. Here, we use voltammetric microelectrodes to quantify the *in situ* concentrations of redox-active species at high vertical resolution (mm to cm) in the benthic porewaters of an oligotrophic Arctic lake (Toolik Lake, AK, USA). Mn(II), Fe(II), O_2, and Fe(III)-organic complexes were detected as the major redox-active species in these porewaters, indicating both Fe(II) oxidation and reductive dissolution of Fe(III) and Mn(IV) minerals. We observed significant spatial heterogeneity in their abundance and distribution as a function of both location within the lake and depth. Microbiological analyses and solid phase Fe(III) measurements were performed in one of the Toolik Lake cores to determine the relationship between biogeochemical redox gradients and microbial communities. Our data reveal iron cycling involving both oxidizing (FeOB) and reducing (FeRB) bacteria. Additionally, we profiled a large microbial iron mat in a tundra seep adjacent to an Arctic stream (Oksrukuyik Creek) where we observed Fe(II) and soluble Fe(III) in a highly reducing environment. The variable distribution of redox-active substances at all the sites yields insights into the nature and distribution of the important terminal electron acceptors in both lacustrine and tundra environments capable of exerting significant influences on the carbon cycle.

Environmental significance

Voltammetric microelectrode measurements were coupled to genomic sequencing to profile the distribution of redox-active species with high vertical resolution in Arctic lacustrine sediment porewaters. Our data are the first high spatial resolution measurements of redox species in an Arctic aquatic environment coupled to the composition of the native microbial community.Distribution of redox-active species in lake sediments and a tundra seep was spatially variable, indicating that microbial abundances are closely coupled to the type and abundance of terminal electron acceptors (TEAs). Knowing the benthic distribution of redox-active TEA species and the responsible microbial communities provides critical information on biogeochemical processes that influence the cycling of carbon, especially in the Arctic, which is disproportionally affected by climate change.

Introduction

Benthic processes in lacustrine environments of the Arctic are pivotal in controlling important biogeochemical processes such as the emission of CO_2,[1,2] and methane;[3–5] metal and nutrient cycling;[6,7] and contaminant attenuation.[8] Redox active species, such as Fe(III), play an important role as terminal electron acceptors (TEA) in organic matter mineralization in lacustrine sediments given their ability to exert influences on methanogenesis if sufficiently abundant for utilization by Fe-reducing microorganisms.[9,10] Fe(III) reducing bacteria can suppress methane production by outcompeting methanogens due to the thermodynamic favorability of using Fe(III) as a TEA as opposed to less energetic TEAs used in methanogenesis.[9,10] Similarly, organic matter oxidation by other TEAs such as oxygen and Mn(IV) solids may also influence the cycling of carbon in Arctic lakes by acting as an alternative electron acceptor.[11,12] Conversely, enzymatic activity by aerobic microbes or abiotic reactions involving oxygen and Fe(II)-mediated (Fenton) pathways may promote organic matter mineralization, enhancing methanogenesis.[1,13–15]

Currently, little is known about the spatial distribution and abundances of important redox active species in sediment porewaters from Arctic lacustrine systems due to the logistical challenges of conducting measurements in these remote and extreme environments. Previous studies in the Arctic that measured the spatial distribution and abundance of redox-active species have indicated great heterogeneity of TEA

[a]*Department of Civil and Environmental Engineering, University of Delaware, Newark, Delaware 19716, USA. E-mail: yochin@udel.edu*

[b]*Bigelow Laboratory for Ocean Sciences, East Boothbay, Maine, 04544, USA*

† Electronic supplementary information (ESI) available. See DOI: 10.1039/d1em00505g

distribution and methane generation between lakes and within lakes that make it difficult to understand carbon cycling on larger scales.[5,9–12] Further, these data rely upon the analysis of redox sensitive substances using *ex situ* methods, which are invasive, reflect a composite sample from specific depth intervals, and are subject to the alteration of native redox conditions, especially when transported outside the field location.[12,16,17] As such there exists very sparse benthic porewater redox data for Arctic lacustrine environments due to their inaccessibility, and a significant knowledge gap remains with respect to the spatial distribution of key redox-active species such as iron, sulfur, and manganese. Given the important role of Arctic lacustrine environments in carbon cycling and the disproportionate way this region is affected by a rapidly warming climate, understanding biogeochemically mediated redox processes will advance our understanding of the carbon cycle in the Arctic.

Voltammetric microelectrodes have been used to measure redox-active species in a broad range of marine and estuarine environments ranging from the water column and sediments[18,19] to hydrothermal vents.[20–22] They have been less commonly applied in lacustrine systems and/or coupled to concurrent microbial analyses of the sediments.[23–28] These complementary approaches could help link the observed porewater geochemistry of TEAs to the microbial activity responsible for the observations. Voltammetric microelectrodes are advantageous because they can achieve high vertical resolution (mm to cm scale) in both sediment cores and the overlying water, while minimally disturbing the sample matrix.[26–29] Additionally, they can quantify multiple redox-active species (*e.g.*, O_2, Fe(II), Mn(II), reduced sulfur species), and identify Fe(III)-organic complexes that exist as stable chelates under reducing conditions simultaneously without or minimally altering their native oxidation states.[18] This enables us to rapidly analyze and quantify porewater chemical species as a function of depth and, more importantly, measure the redox-active species in their *in situ* redox state.[18,22,23,28,29] Finally, microelectrodes are robust, relatively inexpensive, and can be coupled with Bluetooth enabled portable, battery-operated potentiostats. These attributes make this system amenable to a wide variety of field applications.[18,20,22,27,29]

Our goal was to quantify redox-active species associated with O_2, Mn and Fe TEA in high, vertical spatial resolution (mm) in Toolik Lake sediment porewater and a microbial iron mat adjacent to the Oksrukuyik Creek (both in Arctic Alaska). Further, we coupled our voltammetric measurements with 16S rRNA gene sequencing to assess how geochemical gradients are influenced by the composition of the microbial communities at our sites. We hypothesized that shallow cores near the perimeter of Toolik Lake would exhibit different redox species distributions (*i.e.* TEAs) than deeper sediments, based on evidence from previous studies that indicate increased organic matter loading around the Toolik Lake perimeter.[30,31] High-resolution *in situ* measurements of TEAs along geochemical gradients coupled to genomic analyses across various lacustrine environments enable us to better understand the linkages between biogeochemical redox processes and the cycling of carbon.

Materials and methods

Field sampling and experiments

Sediment cores were collected at Toolik Lake, Alaska (68°38′N, 149°43′W, elevation 760 m), an Arctic Long Term Ecological Research (LTER) and National Ecological Observatory Network (NEON) site (Fig. 1a and b). The Toolik Lake watershed lies north of the Brooks Range and is characterized by continuous permafrost with a shallow (~50 cm) active layer. Due to low temperatures and input of nutrients, Toolik Lake is oligotrophic, supporting slow rates of organic matter deposition and decomposition with sediments rich in manganese and iron.[12] Cores collected (6) were divided into shallow cores (STL9, STL10, NETL8, ETL10) *vs.* two paired deep lake cores from the same site (STL15) (Fig. 1 and S6†). Cores from two sites, one in shallow (9 m) water (STL9) and deeper (15 m) water (STL15) were taken from the southwest side of Toolik Lake and are the focus of our study.[12] Coring was conducted from a boat using a gravity corer (Pylonex AB) with a polycarbonate core liner. Following core recovery, cores were transferred to a shore-side laboratory at Toolik Field Station (TFS) and partially extruded until at least 3 cm or more of water was left at the top of the core to preserve the sediment–water interface (SWI), and for placement of the counter and reference electrodes (Fig. S1†).

Redox profiling of an iron seep adjacent to the Oksrukuyik Creek (Fig. 1b and c.) was conducted *in situ* at the site. Steel supports were laid across the ~0.75 m wide and 0.8 m deep pool of water (Fig. S2†). A ring-stand was placed on the platform and supported both a potentiostat (details provided below) and a micromanipulator (Narishige), which held an Hg/Au-amalgam working electrode (description below and Fig. S3†). The counter and reference electrode were securely fastened to the platform with electrical tape so that they were held in the surface water. A Bluetooth connection enabled communication between the potentiostat (Metrohm DropSens μStat-400) and the controlling computer, which optimized working conditions. Water column parameters were measured with a hand-held field multimeter (O_2, pH, temperature, conductivity; YSI). The O_2 electrode was calibrated with a two-point calibration curve using 100% air saturated lake water and a 0% O_2 solution of 1 M sodium ascorbate and NaOH. The pH probe was calibrated using a 3-point calibration curve of certified pH buffers at pH 4, 7, and 10.

Voltammetric analyses

Electrochemical scans were completed using the potentiostat coupled to a three-electrode configuration comprised of a gold–amalgam (Hg/Au) working electrode, Ag/AgCl reference electrode (BASi, West Lafayette, IN), and Pt-wire counter electrode (BASi). Working electrodes were fabricated in our laboratory at the University of Delaware and are identical to ones used in earlier marine studies.[22] Based on previous sediment work in our group,[27] we opted to use PEEK-based material for our microelectrode sheath fabrication, which is much more robust and easily transported to our remote field site than capillary glass microelectrodes. Calibrations for O_2, Mn(II), and Fe(II) were done in unfiltered Toolik Lake water prior to use in the

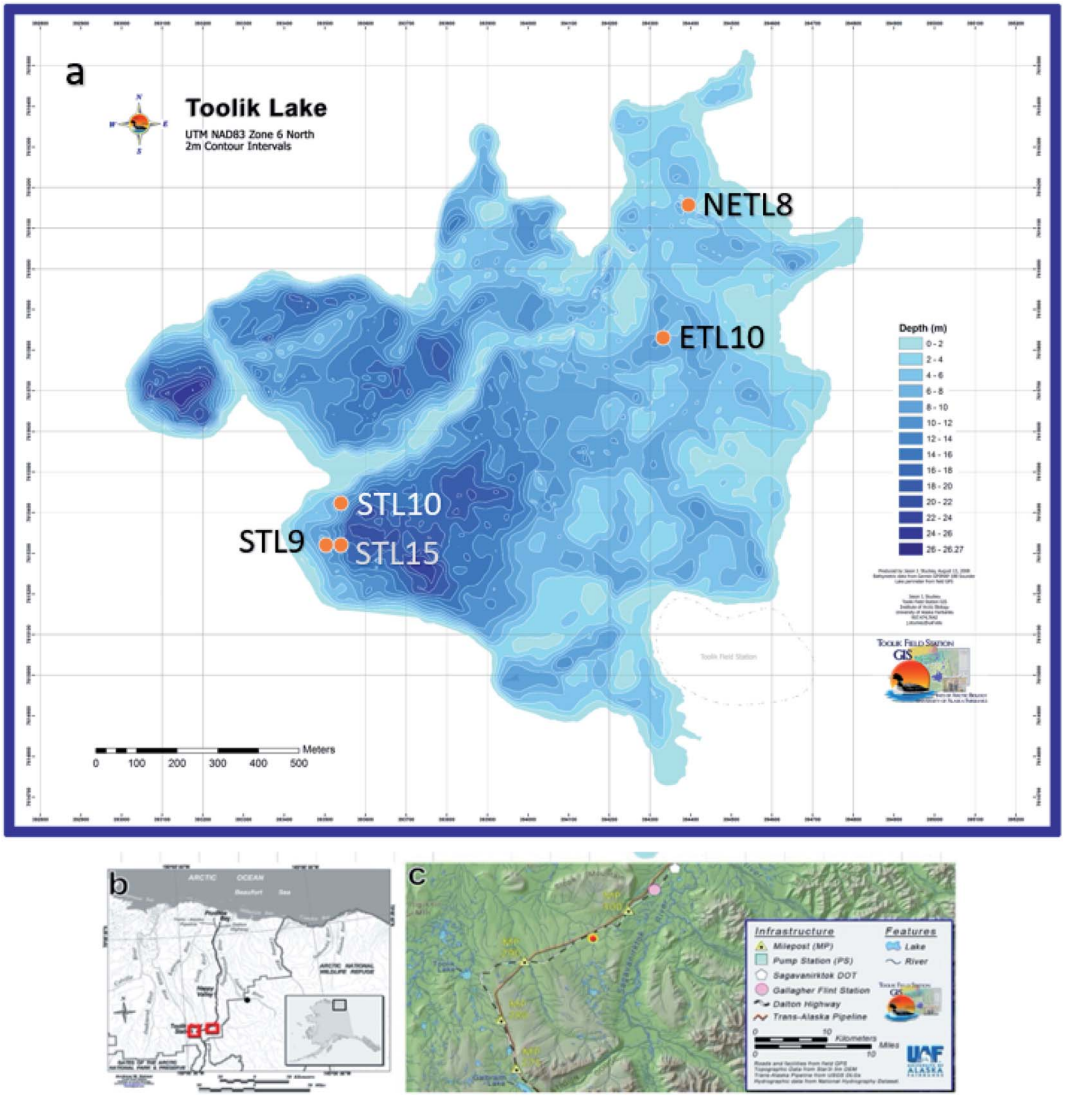

Fig. 1 Bathymetry map of Toolik Lake and sampling locations near Toolik Lake research field station (a). Overview of the North Slope of Alaska, showing the location of Toolik Lake in the left square and the Oksrukuyik Creek iron seep site in the right red square (b), with a detailed view of the Oksrukuyik Creek iron seep site within the Oksrukuyik watershed (c).

field. Details regarding the construction and calibration of the electrodes can be found in the ESI.† Both Ag/AgCl reference and Pt counter electrodes were attached along the top of the core liner so that they were submerged into the overlying water above the sediment interface (Fig. S1†). The Hg/Au–amalgam working electrode was then fastened securely to a micromanipulator above the core liner allowing it to be manually lowered into the overlying water and sediment at mm resolution (Fig. S1†).

Measurements of redox active species in the cores were initiated by placing the working electrode in the overlying water near the sediment/water interface in the core and working down the core in millimeter to centimeter intervals, based on transition areas within biogeochemical gradients, (*i.e.*, higher resolution (mm) measurements were made closer to the SWI, which represents the region of greatest change in redox speciation). At the iron seep, measurements were made in the overlying surface water at centimeter intervals. Near the water–iron mat interface, measurements were made at millimeter intervals into the mat, and then again at larger intervals once the electrode was deeper in the mat.

Scans for both the cores and the iron seep were performed using cyclic voltammetry (CV) at scan rates of 1000 mV s^{-1} from −0.1 V to −1.8 V to −0.1 V (*vs.* Ag/AgCl). A fast scan rate was chosen to increase the sensitivity of the measurement.[18] Three distinct, quantifiable redox-active dissolved species were measured in the cores: O_2, Fe(II), and Mn(II). O_2 occurs at a higher potential (around −0.33 V relative to Ag/AgCl) and presents as the first broad peak on the cathodic scan as it is irreversibly reduced at the amalgam surface of the electrode (Fig. S4A†). Fe(II) and Mn(II) occur at lower potentials around −1.4 V and −1.55 V, respectively, and appear as broad shoulders as they are reduced and deposited onto the electrode surface (Fig. S4B and D†). For Fe(II) and Mn(II) measurements deeper in the core, conditioning steps were employed by holding the

working electrode poised at −0.8 or −0.7 V for 10 to 40 seconds to remove any previously deposited redox active species. Conditioning steps were not used for O_2 measurements, as potentials lower than −0.1 V would partially reduce O_2 to form reactive oxygen species (ROS).[18] The limit of detection for O_2, Mn(II), and Fe(II) with our electrodes was 3, 5, and 5 μM, respectively. Depending on the location and redox-state of the core, other redox-active species were present, including Fe(III)-organic complexes that occurred as broad peaks at higher potentials ranging from −0.1 to −0.8 V (Fig. S4C and D†). Fe(III)-organic signals could not be calibrated, as the specific complexes responsible (mostly oxygen-containing, carboxylate-type ligands) for the signal are unknown.[18,19,22,32] We did not detect any reduced sulfur substances in any of the samples, which most commonly can include H_2S that shows a peak at −0.6 V in voltammograms, and $FeS_{(aq)}$ in the form of molecular clusters, which occurs as a shoulder at −1.15 V.[19] This is not surprising, as Toolik Lake and its watershed is generally devoid of sulfur.[12] Reduced sulfur species have been shown to decrease or eliminate voltametric Fe(III)-organic signals *via* reduction in strongly reducing conditions.[32] Scans were performed 4 to 5 times at each discrete depth, and total analysis time for one depth was about 1 to 3 minutes.

Ex situ iron analysis

Ex situ measurements of Fe(II) concentrations from the iron seep were made from the overlying water collected using a Rhizon membrane filter (0.2 μm) sampling device. This measurement was made to compare the voltammetric assays to more common *ex situ* methods (ESI; Fig. S5†).[17] The 5 cm long filter section of the Rhizon was placed vertically in the top 5 cm of the water overlying the Fe(III)-oxide mat of the iron seep. The water was pulled through the Rhizon by connecting a 10 mL syringe and applying a vacuum. The first 0.2 mL of water was used to rinse the Rhizon and discarded, then 2 mL of water was allowed to flow into the syringe. After the 2 mL sample was collected into the syringe, 1 mL of water was immediately transferred to 0.1 mL of 10 M HCl to yield a ∼1 M HCl and a low pH sample matrix thereby preventing any further oxidation of Fe(II).[33] The Ferrozine assay[34] was used to quantify Fe(III) and Fe(II). Briefly, samples for Fe(II) were combined 1 : 1 with the Ferrozine reagent and quantified using a 6-point standard curve. Fe(III) was calculated by measuring the total Fe in the sample by pre-treating a separate aliquot 5 : 1 with 10% hydroxylamine hydrochloride for 30 min in the dark. Total iron was calculated from a separate 6-point standard curve and Fe(III) calculated as the difference between Fe(II) and total Fe. We did not collect porewaters from our Toolik Lake sediment cores for Fe(II) analysis, as our liners lacked the predrilled ports needed for the Rhizon samplers.

The pool of solid-phase, microbially-reducible Fe(III)-oxides was quantified by adding a known amount of Toolik Lake sediment to a 15 mL centrifuge tube, then adding 5 mL of 0.5 M HCl and incubating at room temperature (21 °C) on a shaker table (30 rpm) for one hour in the dark.[16] After one hour of incubation, the tubes were centrifuged at 3600×*g* for 5 min at 10 °C to pellet the sediment. One milliliter of supernatant was pipetted into a clean 2 mL centrifuge tube. The Ferrozine assay was used to quantify the Fe(II) and Fe(III) in the extraction solutions.[34] All reagents for the Fe extractions were made with glassware that was washed with 2% oxalic acid, then 1% HCl, and rinsed six times in distilled deionized water. The handling of sediment during the extraction process was conducted inside a portable glove bag flushed three times its volume with N_2.

Microbiological sampling and molecular analysis

A separate, paired core at site STL15 was sampled and analyzed for the consortium of microbiological communities associated with redox gradients present in the porewaters. The overlying water was pipetted off the top of the sediment core and the sediment core was extruded until the sediment surface was even with the top edge of the core liner. The surficial orange flocculant layer was pipetted into a 15 mL sterile tube using a sterile cut-off pipette tip and immediately frozen at −20 °C. The core was then extruded upward 0.5 cm and sediment was collected from the center of the core using a metal spatula flame-sterilized with 100% ethanol. Again, the sediment was placed in a 15 mL sterile tube and frozen immediately at −20 °C. This process was repeated for the 1–1.5, 2–2.5, 3–3.5, 4–4.5, 5–5.5, and 6–6.5 cm depth intervals. The microbial iron mat along the banks of the Oksrukuyik Creek was sampled using a sterile 25 mL serological pipette to aspirate the top 1 cm of mat material, which was then transferred into a 15 mL sterile tube and frozen. Samples were shipped frozen (−20 °C) to the Bigelow Laboratory for Ocean Sciences. DNA was extracted using the DNeasy PowerSoil Kit (Qiagen) with slight modifications for the high iron content of these sediments.[7] Briefly, 200 μL of bead beating solution was pipetted out of each bead beating tube, then 0.25 mL of thawed sediment was pipetted with a cut-off pipette tip into the bead beating tube along with 200 μL of phenol–chloroform–isoamyl alcohol (PCI; 25 : 24 : 1). The manufacturer's protocol was followed after the addition of PCI. Extracted DNA was stored at −20 °C until it was sent to Integrated Microbiome Resources (Dalhousie University, Halifax, Nova Scotia, Canada) where it was amplified with the 515F/926R primer pair (V4–V5 region of the 16S rRNA gene sequence) before 250 bp paired-end Illumina sequencing. Raw sequences were assembled, quality controlled, clustered, and classified using mothur.[35] Specifically, assembled sequences with ambiguous bases, homopolymers longer than 8 nt, or those contigs with more or less base pairs than expected from the primer pair were discarded. Chimeric sequences were removed with VSEARCH. Clustering of operational taxonomic units (OTU) was done at the 97% similarity level. All samples were subsampled to the lowest number of sequencing reads (n = 21 264) of the samples in this dataset. Taxonomic assignment of each OTU was made using the SILVA database v138 (release date 16 Dec 2019),[36] curated for the specific region of the 16S rRNA gene sequence used here (V4–V5). We collated OTUs that were taxonomically-assigned to families which contained known iron-oxidizing and iron-reducing bacteria, methanogenic archaea, and methane-oxidizing microorganisms. Then, the

relative abundances of these functional groups were summed within each depth interval. Please see the GitHub website (https://github.com/abmichaud) for the mothur and R code used to process sequence data. These sequence data are deposited in the short read archive under project accession number PRJNA658085 and PRJNA769663.

Results and discussion

Redox active species in Toolik Lake sediment porewaters

We observed O_2, Mn(II), Fe(II), and Fe(III)-complexes in Toolik Lake porewaters in our CV scans from all our cores (Fig. 2 and S4, S6†), indicating both Fe(II) oxidation, as well as nonreductive dissolution of Fe(III) solids, and reductive dissolution of Fe(III) and Mn(IV) solids.[23] In all cores, voltammetric O_2 peaks were distinctly visible around −0.33 V in the water column above the SWI (Fig. S4†). O_2 concentrations vary from saturation (~280 μM) in the overlying water of each core to below the detection limit within the first millimeter to centimeter of depth in sediments (Fig. 2 and S6†). We did not detect any of the reduced metal species (Fe(II) or Mn(II)) in the overlying water of any core (Fig. 2 and S6†) and found little or no vertical overlap between O_2 and reduced metals (Fe(II) and/or Mn(II)) in all cores, which indicates degradation of organic matter by alternate TEAs with increased depth and decreasing favorable free energy, which supports established sediment diagenesis models.[37] Analysis of all cores show that shallow cores located near the lake perimeter (STL9, STL10, NETL8) were highly reducing with little to no O_2 detected below the SWI and more diversity of reduced metals with core depth, while deeper sites and/or cores located further from the shore (STL15, ETL10 respectively) revealed greater O_2 penetration and somewhat less diversity in the reduced metal concentrations as a function of sediment depth (Fig. S6†). Further, at the shallow Toolik STL9 site, O_2 concentrations in the water column *above* the sediments (at ~12 mm above the SWI) were slightly undersaturated (<200 μM: Fig. 2a) while oxygen levels in the deep water site were at or close to saturation (Fig. 2). At the sediment water interface of STL9 (2 mm above to the interface), O_2 decreased approximately 87.5 μM mm^{-1} as a function of depth. This rapid decrease in O_2 concentration below the SWI suggests higher inputs of allochthonous organic matter from the lake perimeter, as observed by others.[5,12,30,31] Further, based upon the reported very low rates of sedimentation observed in Toolik Lake (from a few to <8 mg per cm^2 per year)[11] we believe that inputs of additional metal oxides and organic matter from the pelagic zone to sediments does not fuel this consumption of dioxygen at the SWI. Finally, O_2 did not decrease as noticeably (14.3 μM mm^{-1}) in STL15, suggesting that the organic matter at our deeper site is less abundant and/or more refractory in composition.

Fe(II) and Mn(II) voltammetric peaks occurred at a potential of −1.43 V and −1.55 V, respectively, in the reduced porewaters

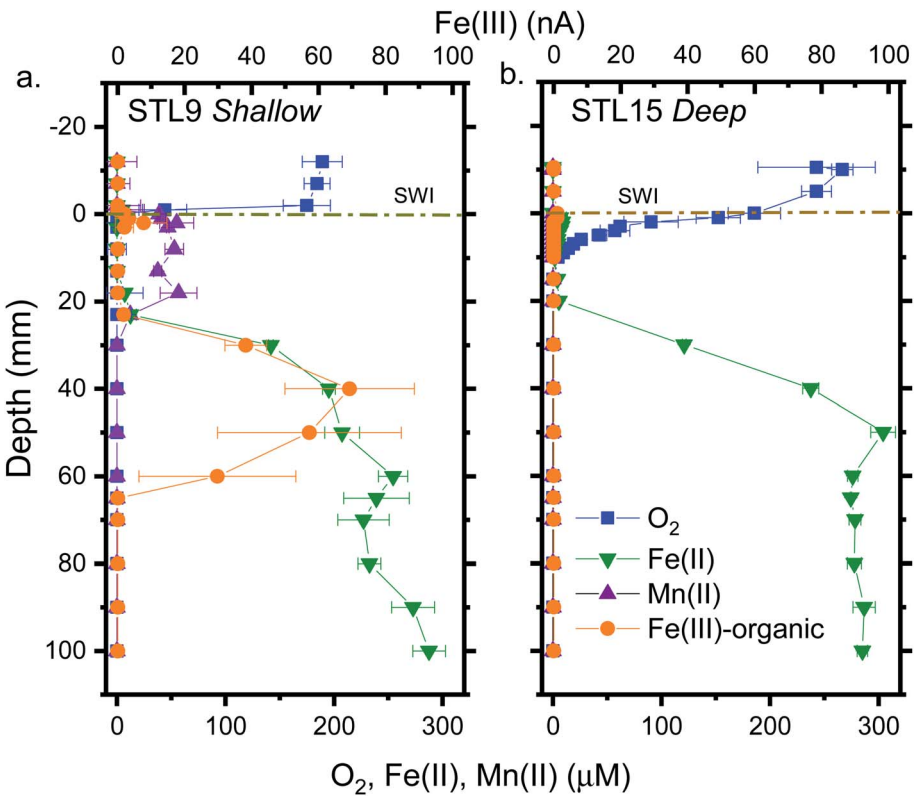

Fig. 2 Profiles of O_2, Mn(II), Fe(II), and Fe(III)-organic complexes (Fe(III)-organic) in (a) STL9 and (b) STL15 from Toolik Lake. Note that Fe(III) is plotted only as an average of current response (nA) that is represented on the top *x*-axis. No error bars were included for current response. For all other species, error bars represent one standard deviation from the mean of three or more measurements and are sometimes smaller than the data point font size. The sediment water interface is abbreviated SWI.

(Fig. S4†). Fe(II) and Mn(II) distributions in these sediment porewaters correspond to their expected free energies whereby manganese oxides are more thermodynamically favorable relative to iron oxides.[37] In STL9 Mn(II) appears in the surficial (~20 mm) sediment, and porewater Mn(II) concentrations increased from 0 to 39 μM at the SWI, reached a maximum of 57 μM at 18 mm of depth in the sediment, then sharply decreased to below the detection limit through the rest of the core (Fig. 2a). While the decrease in Mn(II) is similar to sediment porewater profiles observed in other freshwater lakes,[23,38] it is surprising given that there are no known sinks for Mn(II) under anoxic conditions below where Mn(III) can exist as organic complexes.[39] Carbonates at Toolik Lake are not present in sufficient quantities to influence the precipitation of the major redox species under reducing conditions.[40] One possible explanation is that diffusing Mn(II) from deep sediments accumulates near the SWI (upper 20 mm), as deeper O_2 penetration can act as a barrier for Mn(II) diffusion. Further, Mn(II) has slower oxidation rates with O_2 thereby facilitating accumulation in this sediment zone.[23,38] Because we are close to the limit of detection for Mn(II) in this core (~5 μM) we suspect that Mn(II) is present, but in quantities not detectable by our microelectrode. Mn(II) was also detected at much higher concentrations in the other shallow sediment cores (ESI Fig. S6†). In contrast to STL9, Mn(II) concentrations increased with depth, but concentrations varied widely (from 10's up to 800 μM) and reflects the heterogenous nature of TEA in the sediments of Toolik Lake.

Fe(II) was not present at detectable concentrations in the top cm of STL9 but increased significantly in concentration downcore. Concurrent low Fe(II) concentrations in the presence of Mn(II) in the top cm of STL9 could indicate inorganic Fe(II) oxidation by MnO_2, which would lead to the formation of fresh Fe(III)-oxides.[23] Additionally, a broad Fe(III) peak occurred at potentials ranging from −0.4 to −0.8 V and corresponds to Fe(III)-organic complexes (Fig. S4†). The presence of these Fe(III)-organic complexes has been observed in anoxic sediment porewaters of both estuarine and freshwater wetlands and is attributable to the existence of organic ligands capable of stabilizing Fe(III) under reducing conditions.[41–43] Because we could not quantify the Fe(III)-organic complexes due to the unknown composition of the responsible ligands, the values are reported as current generated (nA). These ligands are presumably comprised of functional groups (*e.g.*, carboxylates and phenolates) known to stabilize Fe(III) under anaerobic conditions[43] and are ubiquitous in dissolved organic matter (DOM).[44–46] Surprisingly, these Fe(III)-organic complexes were not observed in every core (ESI Fig. S6†), which again reflects the highly heterogeneous spatial nature of benthic porewater redox species, and it is unclear what biogeochemical processes control the existence of these Fe(III) stabilizing ligands.

In the only deep water core sample taken (STL15 Toolik located off the western shore of the lake), O_2 and Fe(II) were the only redox-active species detectable (Fig. 2b), although it is possible that Mn(II) existed below our electrode detection limit. O_2 in the water column decreased from 280 μM in the overlying water to 200 μM at the SWI, but unlike STL9, O_2 was observed *below* the sediment–water interface in the first 10 mm of the sediment column after which it became anoxic. Indeed, at this site the surface sediment had a distinctly orange hue, which is likely due to the presence of iron oxides (Fig. 3b and S7†). Fe(II) was present at detection limit concentrations (~5 μM) a few millimeters below the SWI. Fe(II) concentrations did not increase until 20 mm depth suggesting that the presence of O_2 in the sediments prevented the net accumulation of Fe(II) in the porewater. However, it is also at these low levels of O_2 (<50 μM) where the formation of reactive oxygen species (ROS) such as the hydroxyl radical ($OH^{\bullet}$) from the reaction with Fe(II) and reduced DOM can occur resulting in the formation of Fe(III)-oxides.[13] Thus, in this 10 mm zone just below the SWI the formation of ROS could play an important role in mediating the oxidation of Fe(II) diffusing from below. Biological iron oxidation is also commonly prevalent in sediments with low O_2;[47] and likely competes against abiotic ROS mediated reactions in Toolik sediments. It is likely, however, that both biological and ROS-mediated iron oxidation concurrently occur in these surface sediments, contributing to the large pool of poorly crystalline, microbially reducible Fe(III)-oxides found in the surface sediments (Fig. 3b). Finally, it is possible that another TEA, such as nitrate, may have inhibited Fe(III)-oxide reduction even though it was not measured for this study. However, given the oligotrophic nature of Toolik Lake, nitrate levels are low and range from ~1 μM to <0.1 μM below the euphotic zone.[48] Thus, below this redox active zone biological-mediated iron reduction presumably occurs and is facilitated primarily by iron-reducing bacteria[28,47] since we observed steadily increasing Fe(II) concentrations, up to 270 μM to 300 μM at 50 mm to 100 mm depth. Fe(III)-organic complexes were not present in any voltammograms of STL15, unlike STL9. As previously mentioned, if the Fe(III)-organic complexes observed in STL9 are of terrestrial organic matter origin, it is possible that organic matter input into deep sediments is much lower or of different quality than near shore environments. Previous reports of organic-rich groundwater and active zones above permafrost discharging into the perimeter areas of Toolik Lake[12,30,31] support this notion and could increase the abundance of ligands that can chelate Fe(III). These subsurface discharges can also be a source for other chemical species (*e.g.*, macro- and micro-nutrients, other dissolved metal species, *etc.*) that may influence the distribution of redox active species into these shallow sediments. It is also possible that weak Fe(III)-organic complexes in this redox active zone are used as an alternative TEA to Fe(III)-oxides.[49,50] As such, the lack of a Fe(III)-organic complex signal at STL15 could be due to the reduction of these weaker complexes by iron-reducing bacteria to below our detection limits, whereas at STL9 stronger Fe(III)-organic complexes ($\log K > 20$) are the result of chelation with a different pool of ligands derived from allochthonous sources that cannot be readily used as a TEA by these same organisms.[49]

Microbiological analysis in Toolik sediments

The second STL15 core was further analysed to link our biogeochemical data to microbial populations that may participate in the cycling of iron, manganese, and carbon in Toolik

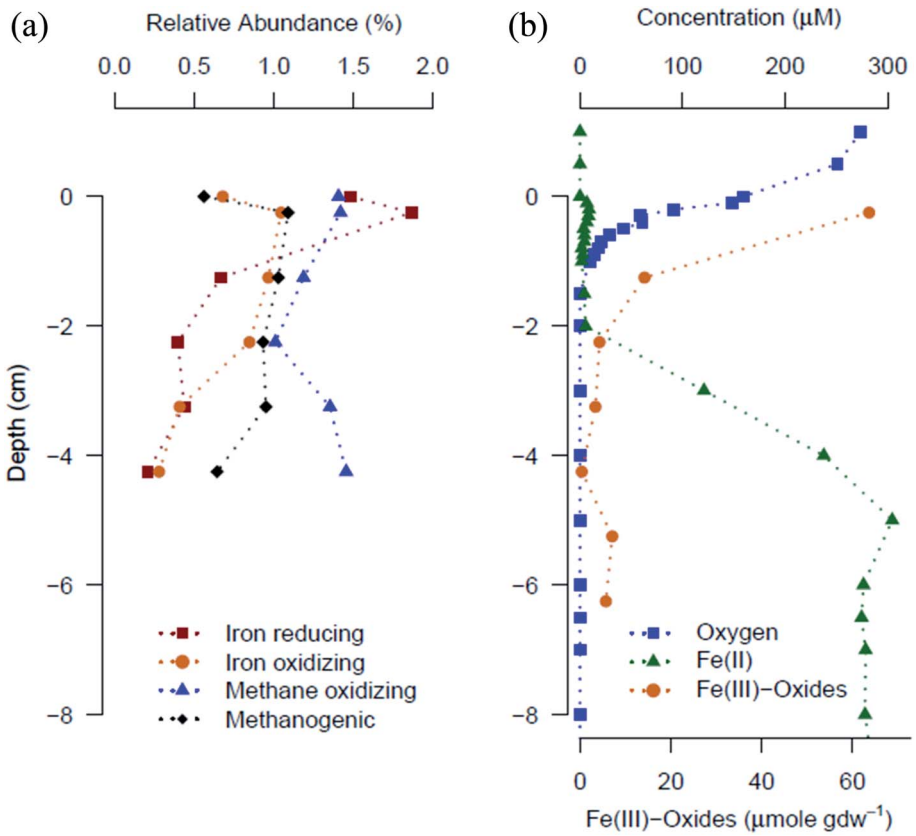

Fig. 3 Relative abundance profiles of key taxa from STL15 containing known iron and methane cycling microorganisms (a) and a zoomed in representation of Fe(II) and O_2 data (b) presented in Fig. 2 (STL15), as well as solid phase measurements of Fe(III) (orange circles). The profiles are summed relative abundances of functional groups of organisms including iron reducing taxa (Geobacteraceae and *Geothrix*), iron oxidizing (Gallionellaceae), methane oxidizing (Methylomonadaceae, Methylococcaceae), and methanogenic (Methanoregulaceae). Fe(II) measurements a the SWI are at the limit of detection (5 μM). Fe(III)-oxides measurements are single measurements.

Lake sediment. The presence of an orange floc on the upper 2 mm of STL15 sediment (Fig. S7†) suggests the presence of Fe(III)-oxides and the possible presence of Fe-oxidizing bacteria (FeOB). Indeed, Fe(III)-oxide measurements of solid-phase minerals in STL15 indicated an abundance of highly reactive Fe(III)-oxides near the surface of the sediment (Fig. 3b) and putative iron-cycling families of bacteria were relatively abundant (based on relative abundances of taxa that can cycle iron or methane) in the surficial sediment, but decreased with depth (Fig. 3a). We found taxa related to known FeOB (Gallionellaceae) at a relative abundance of 0.7% at the SWI, which increased slightly to a peak relative abundance of 1% at 0.25 cm (Fig. 3a). These FeOB then decreased in abundance with depth to <0.4%, concurrent with a loss of the visible Fe(III)-oxides, and extractable, highly-reactive, solid-phase Fe(III)-oxides concentrations (Fig. 3b). The other well-known, freshwater FeOB, *Leptothrix*, was not an abundant member (<0.01%) of the microbial community in the Fe-oxidation region of these sediments. Microbial taxa with relative abundances >1% are generally considered abundant members of the microbial community, while those with relative abundance <0.01% are generally considered rare.[51–53]

The Fe-reducing bacteria (FeRB) bacteria (*Geobacter*, *Geothrix*, *Anaeromyxobacter*, *Desulfuromonas*) were more abundant than the Fe-oxidizing bacteria (*Gallionella*, *Sideroxydans*, *Leptothrix*) in the surficial sediment. These profiles of FeRB were driven by the relative abundances of the *Geobacter* genus, which peak (1.1%) at 0.25 cm depth, then decreased quickly donwcore, but maintained a relative abundance >0.05% (Fig. 3). The genus of the FeRB, *Geothrix*, was also present in greatest relative abundance (0.6%) at 0.25 cm, then decreased downcore. The Gallionellaceae family is known to contain microaerophilic FeOB that tightly follows the oxygen-Fe(II) redox interface.[28,54] In order to sustain FeOB activity there must be a source of Fe(II), which appears to be spatially separated from the obvious Fe(II) source at depth (~5 cm). The Fe(III)-oxides decrease with depth, but the lack of Fe(II) increase until 2 cm depth reveals an apparent imbalance. This imbalance may be caused by loss of Fe(II) as a result of fast abiotic and biotic oxidation in the water column as well as Fe(III)-oxides acting as a sink and adsorbing Fe(II).[55] The low Fe(II) concentrations captured in the upper 2 cm by the high resolution porewater data also imply that there is iron cycling on the surface of the Toolik Lake sediments between biological Fe(III)-oxide reduction that is fueled by coupled biotic and abiotic Fe(II) oxidation. This cycling of iron within biogenic Fe(III)-oxides is known to occur in laboratory experiments which mimic the conditions found in lake sediments,[56] as well as in natural iron mats.[57] The low concentration

of Fe(II) at our voltammetric detection limit within the orange floc at the sediment surface (Fig. 2b and 3b) and within the pool of highly reactive Fe(III)-oxides suggests this process and is likely due to the relatively abundant population of FeRB present. Members of the *Geobacter* genus are known to be primarily obligate anaerobic organisms, so their abundance in the oxic, surficial 0.5 cm with O_2 concentrations in the range of 40–160 μM is noteworthy. There is evidence that *Geobacter sulfurreducens* can grow with oxygen as the sole terminal electron acceptor,[58] but our sequencing of the V4–V5 region of the 16S rRNA gene sequence precluded taxonomic assignments to the species level. Furthermore, the relative abundance of *Geobacter* decreased with depth as the sediment became anoxic and Fe(II) concentrations increased (below 1.5 cm). The presence of *Geobacter* in the oxic, surficial sediment is likely due to the geochemical conditions promoting Fe-reduction such as, fresh, labile organic matter settling to the sediment surface and the presence of a poorly crystalline, energetically favorable Fe(III)-oxide produced by FeOB (Fig. 3). Given the high quantity of Fe(II) in the porewater of Toolik Lake sediments (Fig. 2), the habitat for the FeOB–FeRB consortia may be widespread across the Toolik Lake sediment surface. Since these consortia are present in Fe(III)-oxide rich layers, they may play a significant role in organic matter remineralized through Fe(III) reduction instead of its conversion to methane, especially in deep water sites where FeOB produce highly reactive Fe(III)-oxides for FeRB.

A potential for methanogenesis is indicated throughout the sediment core with the identification of putative Methanogenic families of archaea (*Methanobacteriales*, *Methanococcales*, *Methanomicrobiales*, *Methanosarcinales*, *Methanopyrales*)[59] in uniform abundance from 0.5 to 1% down the entire core. The depth distribution of methanogenic taxa is primarily driven by the genus *Methanoregula*, which is known to be capable of metabolic activity and methanogenesis in acid conditions.[60] Based on our voltammetric data, this possibly indicates that methanogens near the sediment water interface are able to persist on H_2 and CO_2 generated from organic matter mineralization coupled to Fe(III) reduction (or abiotic reduction of Mn(III,IV)).[61] Indeed, measured methogenic communities increased in abundance concurrently with Fe-reducing communities in the upper mms of STL15 sediment (Fig. 3a and b). While methane itself was not measured in this study and linked to the methanogenic communities, past research observed increases in dissolved methane concentration with depth and occur in Toolik Lake sediment from other deep water sites that are similar to STL15.[62]

Putative methane oxidizing bacteria are also present within STL15 sediment. The combination of putative methane-oxidizing families (Methylobacteriaceae, Methylophilaceae, Methylomonadaceae, Methylococcaceae, Methylothermaceae, Methylocystaceae, Beijerinckiaceae, Methylacidophilaceae) were abundant in the shallow sediment, persisting at >1.0% relative abundance throughout the sediment core and increase slightly with depth (Fig. 3a). There is the potential for iron-mediated anaerobic oxidation of methane (AOM) in these sediments given the abundance of Fe(III)-oxides produced at the sediment surface coupled to methane production at depth.[59] We found one OTU (OTU00368) that was classified within the Methanoperedenaceae family, which is known to contain a species implicated in anaerobic iron- and manganese-mediated methane oxidation.[58,63–66] OTU00368 peaked in relative abundance (0.1%) at 0 cm depth, then decreased to 0.04% at 0.25 cm, which is within the surficial, flocculant layer of Fe(III)-oxides and corresponds to the layer where highly reactive Fe(III)-oxides were detected. Within the top 0.5 cm, the Methanoperedenaceae would get relatively fresh and thermodynamically-favorable Fe(III)-oxides from authigenic production by abundant FeOB and methane diffusing upwards from depth.[63] A mass balance at STL15 further indicates that solid-phase Fe(III) is in excess of porewater Fe(II) by many orders of magnitude, which shows that favorable conditions for iron-reducing bacteria, as well as methanotrophs using Fe(III), exist (refer to the SI for a sample calculation). The biogeochemical profiles of non-overlapping Fe(II) and O_2 seen at STL15 in Toolik Lake also occur at shallower depths and are observed at STL9 and other sites in Toolik Lake (Fig. S6†). The redox species profiles and 16S rRNA microbial community data corroborates observations made by other investigators in Arctic and sub-Arctic lakes.[67–69] Cumulatively, this implies that iron abundance and cycling coupled with biological methane oxidation, may play a role in regulating the release of methane from the sediments and is occurring over much of the Toolik Lake benthic zone.

Iron cycling in a tundra seep

As a contrast to lake sediment, we investigated an iron-rich, reducing system situated in a pool of water on the banks of the Oksrukuyik Creek (North Slope, Alaska, Fig. 1c), which contained a thick (~20–40 cm) biogenic Fe(III)-oxide mat produced by FeOB (Fig. S2 and S3).† The Gallionellaceae family of FeOB, with a relative abundance 5.1% of the total microbial community in this sample were the dominant group of FeOB in this Fe-oxide mat, similar to the Fe(III)-rich, orange, surficial sediments of Toolik Lake. FeRB from the *Geobacter* and *Geothrix* genera were also present in the Fe-oxide mat at 1.2% relative abundance (Fig. 4b). The co-occurrence of these two functional groups in a Fe(III)-oxide mat from another aquatic habitat indicates that the consortia of FeOB and FeRB potentially fuel an iron cycle within the Fe(III)-oxide mat. Taxa closely related to methane oxidizing microorganisms were found in the Fe-oxide mat at 1.2% relative abundance (Fig. 4b). The small gully was in a low lying-area surrounded by organic-rich soils and characterized by thermokarst topography. It receives water from a small wetland upgradient and discharges downstream into the Oksrukuyik Creek. The gully may also receive groundwater from a large wet sedge meadow located upgradient from the riverbank. These inputs from the surrounding environment likely provide the organic matter needed to fuel Fe reduction. The water within the gully contains dissolved Fe(II) and Fe(III) (the later existing as stable organic complexes per our previous observations). The seep water is also suboxic (O_2 < 1 μM) and possessed circumneutral pH (6.8) (Fig. 4). For these field analyses, we measured O_2 concentrations with a dissolved oxygen

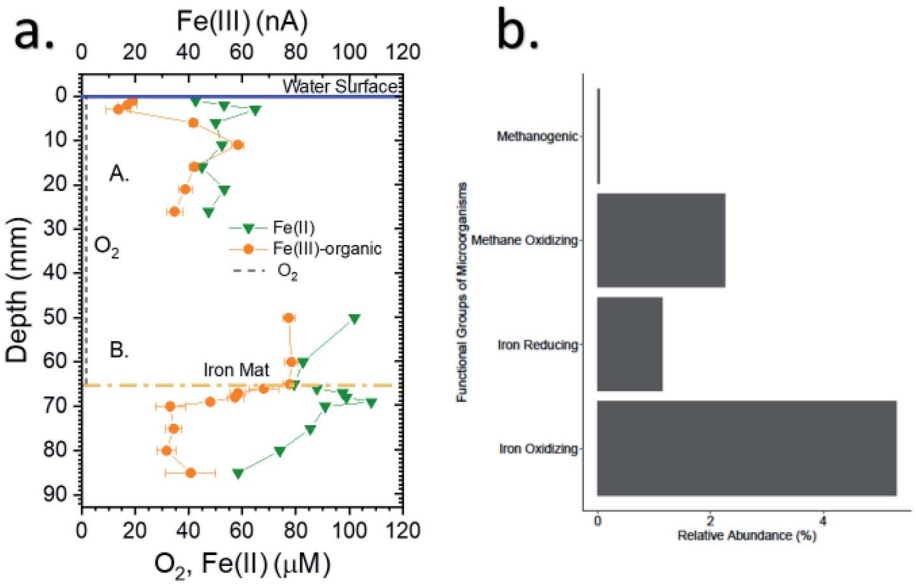

Fig. 4 Fe(II) and Fe(III)-organic complex (Fe(III)-organic) profiles of (A) the water column of an iron seep near Oksrukuyik Creek, located directly above a biogenic iron-oxide mat, and (B) through the biogenic iron–oxide mat (denoted by the brown horizontal dashed line) (a). Note the O_2 concentration is plotted as a vertical dashed line. Fe(III)-organic complex is plotted as an average of current response (nA). Error bars for Fe(III)-organic complex and Fe(II) indicate one standard deviation from the mean of three or more measurements. Abundances of iron and methane cycling bacteria present in iron mat (b). Reported measurements are an aggregate of a sample taken within the iron mat (5 cm vertical resolution) in the water column.

potentiometric electrode, as the voltammetric O_2 peak overlaps with a broad Fe(III)-organic complex signal in these samples, making quantification more difficult. Further, like our measurements in STL9, we reported Fe(III) as current response (nA). Despite the overlying water being suboxic, there were few methanogenic taxa (<0.04%) within the biogenic iron mat (Fig. 4b).

Fe(II) concentrations increase from 41 μM at 1 mm of depth to 62 μM at 3 mm below the surface while the Fe(III)-organic complex current response similarly increases and tracks the Fe(II) profile from 19 nA at 1 mm to 47 nA at 6 mm of depth (Fig. 4). In contrast, an *inverse* profile trend was observed between Fe(II) and Fe(III)-organic complex *within* the microbial iron mat, which occurs between 65 to 70 mm of depth within the mat (Fig. 4). A concomitant increase in the Fe(III)-organic complex signal (nA) with a decrease in Fe(II) concentration at the top of the iron mat may correspond to FeOB communities (*i.e. Gallionella* spp and *Leptothrix ochracea*) consuming Fe(II) through cellular respiration, coupled to the stabilization of generated Fe(III) by strong ligands (*e.g.*, siderophores or DOM).[43,47,70,71] Additionally, biological data indicates that methanogen communities in the iron mat were low in abundance, possibly due to unfavorable thermodynamic conditions where Fe(III) reduction is the dominant redox process. Interestingly, the presence of methane-oxidizing communities in the seep shows that there is the *potential* for methanogenesis and methane removal by AOM in a manner similar to observations in Toolik sediments. While details of our findings of methanogenesis and methane oxidizing communities lie beyond the scope of this paper, they clearly highlight the need for future investigations into this process in lotic and lentic Arctic environments.[72,73]

Environmental implications

To the best of our knowledge, data reported here are the first high vertical resolution *in situ* measurements of redox active substances in Arctic sediment porewaters captured in their native oxidation states coupled to an assessment of the microbial communities as determined by 16S rRNA gene sequencing. Sediment core data from Toolik Lake and an iron mat seep showed spatial variability in redox species, as the iron seep showed reducing behavior (<3 μM O_2) with Fe(II) and Fe(III) species, while sediment cores collected from shallow and deep water depths appeared to have variability in redox-active species with depth (Fig. 2 and S6,† respectively). Microbiological data and solid phase geochemistry in a sediment core at a deep water site illustrate that coupled iron cycling between FeOB and FeRB result in our observed porewater redox species profile and indicates a different cycling pattern in the iron mat. FeRB, aided by the byproduct of FeOB metabolism, may contribute to organic matter mineralization at deeper lake spots within suboxic sediments and suppress methanogenesis. Conversely, shallower areas near the lake perimeter that exhibit slightly more reducing conditions and may be less inhibitory to methanogenesis due to incomplete organic matter mineralization. Future studies from our group at this field site will corroborate voltammetric measurements with pH and other (*e.g.*, methane, DIC, and DOC if possible) measurements.

Our preliminary data in Arctic lacustrine sediments highlights the redox chemistry that results from the unique

environment where they exist. For example, Toolik Lake spends the majority of the year under ice cover, which can promote lower oxygen conditions, and even anoxia, in the water column near the sediment surface, leading to more reducing conditions in the sediment and a potentially higher flux of reduced solutes from sediment.[74] While we are currently unaware of existing Arctic sediment methane measurements under the ice, these reducing conditions could promote methanogenesis.[74,75] Conversely, methanotrophs may persist on alternative electron acceptors (*i.e.* Fe(III)-oxides) during ice-induced low oxygen periods.[75] Although our measurements captured only the ice-free summer behavior of redox-active solutes, it is highly likely that they are influenced by winter hydrodynamics.[74,76,77] Future studies will be paramount in linking winter hydrodynamics, mixing, and hydrology to biogeochemical cycling in order to determine the effect of decreasing ice cover on methane production within Arctic lake sediments. Previous studies have linked methane transport from active layers of permafrost thaw and ground water into near shore, shallow areas of Toolik Lake.[30,31] This implies that Toolik Lake, along with other Arctic lakes, could receive higher loadings of methane in the future as permafrost thaw continues.

This study demonstrates the versatility of utilizing voltammetric microelectrodes in remote field studies, due to the portability and durability of both the electrodes and controlling potentiostat. Voltammetry is a potentially powerful tool to assess how redox reactions in Arctic lacustrine systems impact greenhouse gas production and elemental cycling in the Arctic, which is highly sensitive to climate change.

Conflicts of interest

There are no conflicts to declare.

Acknowledgements

The authors thank George Luther who provided valuable guidance regarding electrode fabrication and data interpretation. Fig. 1 is courtesy of Toolik Field Station GIS department. This research was funded by NSF grants CBET 1804611 (Y. Chin) and DEB/PP 1754358 (D. Emerson). Toolik Field Station (University of Alaska Fairbanks) staff provided necessary logistical support for this research. Lauren O'Connor, William Sutor, and Rémi Massé provided essential fieldwork assistance.

References

1 A. Trusiak, L. A. Treibergs, G. W. Kling and R. M. Cory, The role of iron and reactive oxygen species in the production of CO_2 in arctic soil waters, *Geochim. Cosmochim. Acta*, 2018, **224**, 80–95.

2 S. MacIntyre, A. Cortés and S. Sadro, Sediment respiration drives circulation and production of CO_2 in ice-covered Alaskan Arctic lakes, *Limnol. Oceanogr. Lett.*, 2018, **3**, 302–310.

3 L. Klüpfel, A. Piepenbrock, A. Kappler and M. Sander, Humic substances as fully regenerable electron acceptors in recurrently anoxic environments, *Nat. Geosci.*, 2014, **7**, 195–200.

4 K. M. Walter, S. A. Zimov, J. P. Chanton, D. Verbyla and F. S. Chapin, Methane bubbling from Siberian thaw lakes as a positive feedback to climate warming, *Nature*, 2006, **443**, 71–75.

5 P. B. Matheus Carnevali, M. Rohrssen, M. R. Williams, A. B. Michaud, H. Adams, D. Berisford, G. D. Love, J. C. Priscu, O. Rassuchine, K. P. Hand and A. E. Murry, Methane sources in arctic thermokarst lake sediments on the North Slope of Alaska, *Geobiology*, 2015, **13**, 181–197.

6 B. Braune, J. Chételat, M. Amyot, T. Brown, M. Clayden, M. Evans, A. Fisk, A. Gaden, C. Girard, A. Hare and J. Kirk, Mercury in the marine environment of the Canadian Arctic: review of recent findings, *Sci. Total Environ.*, 2015, **509**, 67–90.

7 D. Emerson, J. J. Scott, J. Benes and W. B. Bowden, Microbial iron oxidation in the arctic tundra and its implications for biogeochemical cycling, *Appl. Environ. Microbiol.*, 2015, **81**, 8066–8075.

8 T. Borch, R. Kretzschmar, A. Kappler, P. V. Cappellen, M. Ginder-Vogel, A. Voegelin and K. Campbell, Biogeochemical redox processes and their impact on contaminant dynamics, *Environ. Sci. Technol.*, 2010, **44**, 15–23.

9 D. A. Lipson, M. Jha, T. K. Raab and W. C. Oechel, Reduction of iron(III) and humic substances plays a major role in anaerobic respiration in an Arctic peat soil, *J. Geophys. Res.: Biogeosci.*, 2010, **115**, 1–13.

10 K. E. Miller, C. T. Lai, E. S. Friedman, L. T. Angenent and D. A. Lipson, Methane suppression by iron and humic acids in soils of the Arctic Coastal Plain, *Soil Biol. Biochem.*, 2015, **83**, 176–183.

11 J. C. Cornwell, PhD thesis, University of Alaska Fairbanks, 1983.

12 J. C. Cornwell and G. W. Kipphut, Biogeochemistry of manganese-and iron-rich sediments in Toolik Lake, Alaska, in Toolik Lake, *Developments in Hydrobiology*, 1992, vol. 78, pp. 45–59.

13 S. E. Page, G. W. Kling, M. Sander, K. H. Harrold, J. R. Logan, K. McNeill and R. M. Cory, Dark formation of hydroxyl radical in Arctic soil and surface waters, *Environ. Sci. Technol.*, 2013, **47**, 12860–12867.

14 M. Keiluweit, P. S. Nico, M. Kleber and S. Fendorf, Are oxygen limitations under recognized regulators of organic carbon turnover in upland soils?, *Biogeochemistry*, 2016, **127**, 157–171.

15 J. L. Wilmouth, J. K. Schaefer, D. R. Schlesinger, S. W. Roth, P. G. Hatcher, J. K. Shoemaker and X. Zhang, The role of oxygen in stimulating methane production in wetlands, *GCB Bioenergy*, 2021, **27**, 5831–5847.

16 K. Laufer, A. B. Michaud, H. Røy and B. B. Jørgensen, Reactivity of Iron Minerals in the Seabed Toward Microbial Reduction–A Comparison of Different Extraction Techniques, *Geomicrobiol. J.*, 2020, **37**, 170–189.

17 J. Seeberg-Elverfieldt, M. Schlüter, T. Feseker and M. Kölling, Rhizon sampling of porewaters near the sediment–water

interface of aquatic systems, *Limnol. Oceanogr.: Methods*, 2005, **3**, 361–371.

18 P. J. Brendel and G. W. Luther, Development of a gold amalgam voltammetric microelectrode for the determination of dissolved Fe, Mn, O_2, and S (–II) in porewaters of marine and freshwater sediments, *Environ. Sci. Technol.*, 1995, **29**, 751–761.

19 G. W. Luther, P. J. Brendel, B. L. Lewis, B. Sundby, L. Lefrançois, N. Silverberg and D. B. Nuzzio, Simultaneous measurement of O_2, Mn, Fe, I^-, and S (–II) in marine pore waters with a solid-state voltammetric microelectrode, *Limnol. Oceanogr.*, 1998, **43**, 325–333.

20 G. W. Luther, T. F. Rozan, M. Taillefert, D. B. Nuzzio, C. Di Meo, T. M. Shank, R. A. Lutz and S. C. Cary, Chemical speciation drives hydrothermal vent ecology, *Nature*, 2001, **410**, 813–816.

21 D. B. Nuzzio, M. Taillefert, S. C. Cary, A. L. Reysenbach and G. W. Luther, *In situ* voltammetry at deep-sea hydrothermal vents, environmental electrochemistry, *ACS Symp. Ser.*, 2002, **811**, 40–51.

22 G. W. Luther, B. T. Glazer, S. Ma, R. E. Trouwborst, T. S. Moore, E. Metzger, C. Kraiya, T. J. Waite, G. Druschel, B. Sundby and M. Taillefert, Use of voltammetric solid-state (micro) electrodes for studying biogeochemical processes: laboratory measurements to real time measurements with an *in situ* electrochemical analyzer (ISEA), *Mar. Chem.*, 2008, **108**, 221–235.

23 S. Ma, G. W. Luther, J. Keller, A. S. Madison, E. Metzger, D. Emerson and J. P. Megonigal, Solid-State Au/Hg Microelectrode for the Investigation of Fe and Mn Cycling in a Freshwater Wetland: Implications for Methane Production, *Electroanalysis*, 2008, **20**, 233–239.

24 L. Smith, M. C. Watzin and G. Druschel, Relating sediment phosphorus mobility to seasonal and diel redox fluctuations at the sediment–water interface in a eutrophic freshwater lake, *Limnol. Oceanogr.*, 2011, **56**, 2251–2264.

25 A. W. Schroth, C. D. Giles, P. D. Isles, Y. Xu, Z. Perzan and G. K. Druschel, Dynamic coupling of iron, manganese, and phosphorus behavior in water and sediment of shallow ice-covered eutrophic lakes, *Environ. Sci. Technol.*, 2015, **49**, 9758–9767.

26 C. D. Giles, P. D. Isles, T. Manley, Y. Xu, G. K. Druschel and A. W. Schroth, The mobility of phosphorus, iron, and manganese through the sediment–water continuum of a shallow eutrophic freshwater lake under stratified and mixed water-column conditions, *Biogeochemistry*, 2016, **127**, 15–34.

27 B. C. McAdams, R. M. Adams, W. A. Arnold and Y. P. Chin, Novel insights into the distribution of reduced sulfur species in prairie pothole wetland pore waters provided by bismuth film electrodes, *Environ. Sci. Technol. Lett.*, 2016, **3**, 104–109.

28 D. J. MacDonald, A. J. Findlay, S. M. McAllister, J. M. Barnett, P. Hredzak-Showalter, S. T. Krepski, S. G. Cone, J. Scott, S. K. Bennet, C. S. Chan and D. Emerson, Using *in situ* voltammetry as a tool to identify and characterize habitats of iron-oxidizing bacteria: from freshwater wetlands to hydrothermal vent sites, *Environ. Sci.: Processes Impacts*, 2014, **16**, 2117–2126.

29 J. M. Hudson, D. J. MacDonald, E. R. Estes and G. W. Luther, A durable and inexpensive pump profiler to monitor stratified water columns with high vertical resolution, *Talanta*, 2019, **199**, 415–424.

30 A. Paytan, A. L. Lecher, N. Dimova, K. J. Sparrow, F. G. T. Kodovska, J. Murray, S. Tulaczyk and J. D. Kessler, Methane transport from the active layer to lakes in the Arctic using Toolik Lake, Alaska, as a case study, *Proc. Natl. Acad. Sci. U. S. A.*, 2015, **112**, 3636–3640.

31 A. L. Lecher, P. C. Chuang, M. Singleton and A. Paytan, Sources of methane to an Arctic lake in Alaska: an isotopic investigation, *J. Geophys. Res.: Biogeosci.*, 2017, **122**, 753–766.

32 M. Taillefert, A. B. Bono and G. W. Luther, Reactivity of freshly formed Fe(III) in synthetic solutions and (pore) waters: voltammetric evidence of an aging process, *Environ. Sci. Technol.*, 2000, **34**, 2169–2177.

33 K. Porsch and A. Kappler, Fe(II) oxidation by molecular O_2 during HCl extraction, *Environ. Chem.*, 2011, **8**, 190–197.

34 L. L. Stookey, Ferrozine-a new spectrophotometric agent for iron, *Anal. Chem.*, 1976, **48**, 1216–1220.

35 P. D. Schloss, S. L. Westcott, T. Ryabin, J. R. Hall, M. Hartmann, E. B. Hollister, R. A. Lesniewski, B. B. Oakley, D. H. Parks, C. J. Robinson and J. W. Sahl, Introducing mothur: open-source, platform-independent, community-supported software for describing and comparing microbial communities, *Appl. Environ. Microbiol.*, 2009, **75**, 7537–7541.

36 C. Quast, E. Pruesse, P. Yilmaz, J. Gerken, T. Schweer, P. Yarza, J. Peplies and F. O. Glöckner, The SILVA ribosomal RNA gene database project: improved data processing and web-based tools, *Nucleic Acids Res.*, 2013, **41**, D590–D596.

37 R. A. Berner, in *Early diagenesis: a Theoretical Approach*, Princeton University Press, 1980, vol. 1.

38 D. Joung, M. Leduc, B. Ramcharitar, Y. Xu, P. D. Isles, J. D. Stockwell, G. K. Druschel, T. Manley and A. W. Schroth, Winter weather and lake-watershed physical configuration drive phosphorus, iron, and manganese dynamics in water and sediment of ice-covered lakes, *Limnol. Oceanogr.*, 2017, **62**, 1620–1635.

39 A. S. Madison, B. M. Tebo, A. Mucci, B. Sundby and G. W. Luther, Abundant porewater Mn(III) is a major component of the sedimentary redox system, *Science*, 2013, **341**, 875–878.

40 T. D. Hamilton, PhD thesis, University of Alaska Institute of Arctic Biology, 2003.

41 G. W. Luther, P. A. Shellenbarger and P. J. Brendel, Dissolved organic Fe(III) and Fe(II) complexes in salt marsh porewaters, *Geochim. Cosmochim. Acta*, 1996, **60**, 951–960.

42 M. Taillefert, V. C. Hover, T. F. Rozan, S. M. Theberge and G. W. Luther, The influence of sulfides on soluble organic–Fe(III) in anoxic sediment porewaters, *Estuaries*, 2002, **25**, 1088–1096.

43 J. A. Hakala, R. L. Fimmen, Y. P. Chin, S. G. Agrawal and C. P. Ward, Assessment of the geochemical reactivity of Fe-

DOM complexes in wetland sediment pore waters using a nitroaromatic probe compound, *Geochim. Cosmochim. Acta*, 2009, **73**, 1382–1393.

44 A. E. Mutschlecner, J. J. Guerard, J. B. Jones and T. K. Harms, Regional and intra-annual stability of dissolved organic matter composition and biolability in high-latitude Alaskan rivers, *Limnol. Oceanogr.*, 2018, **63**, 1605–1621.

45 K. R. Gagné, S. C. Ewers, C. J. Murphy, R. Daanen, K. W. Anthony and J. J. Guerard, Composition and photoreactivity of organic matter from permafrost soils and surface waters in interior Alaska, *Environ. Sci.: Processes Impacts*, 2020, **22**, 1525–1539.

46 E. N. MacDonald, S. E. Tank, S. V. Kokelj, D. G. Froese and R. H. Hutchins, Permafrost-derived dissolved organic matter composition varies across permafrost end-members in the western Canadian Arctic, *Environ. Res. Lett.*, 2021, **16**, 024036.

47 A. Kappler and K. L. Straub, Geomicrobiological cycling of iron, *Rev. Mineral. Geochem.*, 2005, **59**, 85–108.

48 S. C. Whalen and V. Alexander, Seasonal inorganic carbon and nitrogen transport by phytoplankton in an arctic lake, *Can. J. Fish. Aquat. Sci.*, 1986, **43**, 1177–1186.

49 J. R. Haas and T. J. Dichristina, Effects of Fe(III) chemical speciation on dissimilatory Fe(III) reduction by Shewanella putrefaciens, *Environ. Sci. Technol.*, 2002, **36**, 373–380.

50 M. Taillefert, J. S. Beckler, E. Carey, J. L. Burns, C. M. Fennessey and T. J. DiChristina, Shewanella putrefaciens produces an Fe(III)-solubilizing organic ligand during anaerobic respiration on insoluble Fe(III) oxides, *J. Inorg. Biochem.*, 2007, **101**, 1760–1767.

51 B. J. Campbell, L. Yu, J. F. Heidelberg and D. L. Kirchman, Activity of abundant and rare bacteria in a coastal ocean, *Proc. Natl. Acad. Sci. U. S. A.*, 2011, **108**, 12776–12781.

52 M. D. Lynch and J. D. Neufeld, Ecology and exploration of the rare biosphere, *Nat. Rev. Microbiol.*, 2015, **13**, 217–229.

53 R. Props, F. M. Kerckhof, P. Rubbens, J. De Vrieze, E. H. Sanabria, W. Waegeman, P. Monsieurs, F. Hammes and N. Boon, Absolute quantification of microbial taxon abundances, *ISME J.*, 2017, **11**, 584–587.

54 G. K. Druschel, D. Emerson, R. Sutka, P. Suchecki and G. W. Luther, Low-oxygen and chemical kinetic constraints on the geochemical niche of neutrophilic iron(II) oxidizing microorganisms, *Geochim. Cosmochim. Acta*, 2008, **72**, 3358–3370.

55 M. M. Urrutia, E. E. Roden and J. M. Zachara, Influence of aqueous and solid-phase Fe(II) complexants on microbial reduction of crystalline iron(III) oxides, *Environ. Sci. Technol.*, 1999, **33**, 4022–4028.

56 D. Sobolev and E. E. Roden, Evidence for rapid microscale bacterial redox cycling of iron in circumneutral environments, *Antonie van Leeuwenhoek*, 2002, **81**, 587–597.

57 E. Roden, J. M. McBeth, M. Blothe, E. M. Percak-Dennet, E. J. Flemming, R. R. Holyoke, G. W. Luther and D. Emerson, The microbial ferrous wheel in a neutral pH groundwater seep, *Front. Microbiol.*, 2012, **3**, 172.

58 W. C. Lin, M. V. Coppi and D. R. Lovley, Geobacter sulfurreducens can grow with oxygen as a terminal electron acceptor, *Appl. Environ. Microbiol.*, 2004, **70**, 2525–2528.

59 Y. Liu, in *Taxonomy of Methanogens. Handbook of Hydrocarbon and Lipid Microbiology*, Springer-Verlag Berlin Heidelberg GmbH, 2010, pp. 547–558.

60 S. Bräuer, H. Cadillo-Quiroz, E. Yashiro, J. B. Yavitt and S. H. Zinder, Isolation of a novel acidophilic methanogen from an acidic peat bog, *Nature*, 2006, **442**, 192–194.

61 M. Patzner, M. Logan, A. McKenna, R. Young, Z. Zhou, H. Joss, C. Mueller, C. Hoschen, T. Scholten, D. Straub, S. Kleindienst, T. Borch, A. Kappler and C. Bryce, Microbial iron(III) reduction during palsa collapse promotes greenhouse gas emissions before complete permafrost thaw, EarthArXiv, 2021, DOI: 10.21203/rs.3.rs-691992/v1.

62 K. A. Bretz and S. C. Whalen, Methane cycling dynamics in sediments of Alaskan Arctic Foothill lakes, *Inland Waters*, 2014, **4**, 65–78.

63 J. D. Coates, D. J. Ellis, C. V. Gaw and D. R. Lovley, Geothrix fermentans gen. nov., sp. nov., a novel Fe(III)-reducing bacterium from a hydrocarbon-contaminated aquifer, *Int. J. Syst. Evol. Microbiol.*, 1999, **49**, 1615–1622.

64 C. Knief, Diversity and habitat preferences of cultivated and uncultivated aerobic methanotrophic bacteria evaluated based on pmoA as molecular marker, *Front. Microbiol.*, 2015, **6**, 1–38.

65 A. O. Leu, C. Cai, S. J. McIlroy, G. Southam, V. J. Orphan, Z. Yuan, S. Hu and G. W. Tyson, Anaerobic methane oxidation coupled to manganese reduction by members of the Methanoperedenaceae, *ISME J.*, 2020, **14**, 1030–1041.

66 A. Pienkowska, M. Glodowska, M. Mansor, D. Buchner, D. Straub, S. Kleindienst and A. Kappler, Isotopic Labeling Reveals Microbial Methane Oxidation Coupled to Fe(III) Mineral Reduction in Sediments from an As-Contaminated Aquifer, *Environ. Sci. Technol. Lett.*, 2021, **8**, 832–837.

67 N. Riedinger, M. J. Formolo, T. W. Lyons, S. Henkel, A. Beck and S. Kasten, An inorganic geochemical argument for coupled anaerobic oxidation of methane and iron reduction in marine sediments, *Geobiology*, 2014, **12**, 172–181.

68 K. Martinez-Cruz, M. C. Leewis, I. C. Herriott, A. Sepulveda-Jauregui, K. W. Anthony, F. Thalasso and M. B. Leigh, Anaerobic oxidation of methane by aerobic methanotrophs in sub-Arctic lake sediments, *Sci. Total Environ.*, 2017, **607**, 23–31.

69 L. Cabrol, F. Thalasso, L. Gandois, A. Sepulveda-Jauregui, K. Martinez-Cruz, R. Teisserenc, N. Tananaev, A. Tveit, M. M. Svenning and M. Barret, Anaerobic oxidation of methane and associated microbiome in anoxic water of Northwestern Siberian lakes, *Sci. Total Environ.*, 2020, **736**, 139588.

70 D. Emerson and N. P. Revsbech, Investigation of an iron-oxidizing microbial mat community located near Aarhus, Denmark: laboratory studies, *Appl. Environ. Microbiol.*, 1994, **60**, 4032–4038.

71 K. P. Nevin and D. R. Lovley, Mechanisms for accessing insoluble Fe(III) oxide during dissimilatory Fe(III) reduction

by Geothrix fermentans, *Appl. Environ. Microbiol.*, 2002, **68**, 2294–2299.

72 O. Sivan, M. Adler, A. Pearson, F. Gelman, I. Bar-Or, S. G. John and W. Eckert, Geochemical evidence for iron-mediated anaerobic oxidation of methane, *Limnol. Oceanogr.*, 2011, **56**, 1536–1544.

73 O. Sivan, G. Antler, A. V. Turchyn, J. J. Marlow and V. J. Orphan, Iron oxides stimulate sulfate-driven anaerobic methane oxidation in seeps, *Proc. Natl. Acad. Sci. U. S. A.*, 2014, **111**, E4139–E4147.

74 S. C. Whalen and J. C. Cornwell, Nitrogen, phosphorus, and organic carbon cycling in an arctic lake, *Can. J. Fish. Aquat. Sci.*, 1985, **42**, 797–808.

75 R. He, J. Wang, J. W. Pohlman, Z. Jia, Y. X. Chu, M. J. Wooller and M. B. Leigh, Metabolic flexibility of aerobic methanotrophs under anoxic conditions in Arctic lake sediments, *ISME J.*, 2022, **16**, 78–90.

76 J. Jansen, S. MacIntyre., D. C. Barrett, Y. P. Chin, A. Cortés, A. L. Forrest, A. R. Hrycik, R. Martin, B. C. McMeans, M. Rautio and R. Schwefel, Winter limnology: how do hydrodynamics and biogeochemistry shape ecosystems under ice?, *J. Geophys. Res.: Biogeosci.*, 2021, **126**, e2020JG006237.

77 B. C. McAdams, W. A. Arnold, M. J. Wilkins and Y. P. Chin, Ice Cover Influences Redox Dynamics in Prairie Pothole Wetland Sediments, *J. Geophys. Res.: Biogeosci.*, 2021, **126**, e2021JG006318.

